SLC13A5 Is a Novel Transcriptional Target of the Pregnane X Receptor and Sensitizes Drug-Induced Steatosis in Human Liver

Linhao Li, Haishan Li, Brandy Garzel, Hui Yang, Tatsuya Sueyoshi, Qing Li, Yan Shu, Junran Zhang, Bingfang Hu, Scott Heyward, Timothy Moeller, Wen Xie, Masahiko Negishi, and Hongbing Wang

Department of Pharmaceutical Sciences, University of Maryland School of Pharmacy, Baltimore, Maryland (L.L., H.L., B.G., H.Y., Q.L., Y.S., H.W.); Pharmacogenetics Section, Laboratory of Reproductive and Developmental Toxicology, National Institute of Environmental and Health Sciences, National Institutes of Health, Research Triangle Park, North Carolina (T.S., M.N.); Department of Radiation Oncology, Case Western Reserve University, Cleveland, Ohio (J.Z.); Bioreclamation In Vitro Technologies, Baltimore, Maryland (S.H., T.M.); and Center for Pharmacogenetics and Department of Pharmaceutical Sciences, University of Pittsburgh School of Pharmacy, Pittsburgh, Pennsylvania (B.H., W.X.)

ABSTRACT

The solute carrier family 13 member 5 (SLC13A5) is a sodium-coupled transporter that mediates cellular uptake of citrate, which plays important roles in the synthesis of fatty acids and cholesterol. Recently, the pregnane X receptor (PXR, NR1I2), initially characterized as a xenobiotic sensor, has been functionally linked to the regulation of various physiologic processes that are associated with lipid metabolism and energy homeostasis. Here, we show that the *SLC13A5* gene is a novel transcriptional target of PXR, and altered expression of SLC13A5 affects lipid accumulation in human liver cells. The prototypical PXR activator rifampicin markedly induced the mRNA and protein expression of SLC13A5 in human primary hepatocytes. Utilizing cell-based luciferase reporter assays, electrophoretic mobility shift assays, and chromatin immunoprecipitation assays, we identified and functionally characterized two enhancer modules located upstream of the *SLC13A5* gene transcription start site that are associated with regulation of PXR-mediated SLC13A5 induction. Functional analysis further revealed that rifampicin can enhance lipid accumulation in human primary hepatocytes, and knockdown of SLC13A5 expression alone leads to a significant decrease of the lipid content in HepG2 cells. Overall, our results uncover *SLC13A5* as a novel target gene of PXR and may contribute to drug-induced steatosis and metabolic disorders in humans.

Introduction

The tricarboxylic acid (TCA) cycle is central to oxidative metabolism and biosynthesis of fatty acids, glucose, and nonessential amino acids, which are pivotal to the highly coordinated energy homeostasis (Raimundo et al., 2011; Stobbe et al., 2012). The solute carrier family 13 member 5 (SLC13A5) is a newly identified sodium-coupled transporter that mediates the cellular uptake of the TCA intermediate, citrate, which functions as an important precursor in the biosynthesis of fatty acids, isoprenoids, and cholesterol (Inoue et al., 2002c; Gopal et al., 2007). Belonging to the sodium dicarboxylate/sulfate cotransporter (NaDC) family that includes the well characterized NaDC1 and NaDC3 (Pajor, 1995; Chen et al., 1998), SLC13A5 recognizes and transports various dicarboxylate and tricarboxylate TCA intermediates, with citrate holding the highest substrate affinity

(Inoue et al., 2002b). Expression of SLC13A5 is most abundant in the liver, where it controls the uptake of citrate into hepatocytes from the blood stream, in which citrate circulates at a relatively high level ($\sim$150 μM) (Gopal et al., 2007). Consistent with its biologic function, immunostaining demonstrated that the SLC13A5 protein is exclusively expressed in the sinusoidal membrane of hepatocytes in the liver (Inoue et al., 2004). Notably, the blood concentration of citrate is severalfold higher than that of all other TCA intermediates combined, thus SLC13A5 may play key physiologic roles in the generation of metabolic energy by facilitating the utilization of circulating citrate, which would eventually affect pathophysiological conditions such as obesity, type 2 diabetes, and other metabolic disorders (Inoue et al., 2002b; Pajor, 2014). However, despite the postulated importance of SLC13A5 in energy metabolism, whether the expression of this uptake transporter can be perturbed under various drug exposures and how the expression of this gene is transcriptionally regulated are largely unknown.

The pregnane X receptor (PXR, NR1I2) has been characterized as one of the central components in coordinated responses to xenobiotic and endobiotic stimulation by controlling the

ABBREVIATIONS: BODIPY, boron-dipyrromethene; ChIP, chromatin immunoprecipitation; DMSO, dimethylsulfoxide; EMSA, electrophoretic mobility shift assay; GAPDH, glyceraldehyde-3-phosphate dehydrogenase; HPH, human primary hepatocytes; hPXR, human PXR; NaDC, sodium dicarboxylate/sulfate cotransporter; PCR, polymerase chain reaction; PXR, pregnane X receptor; RIF, rifampicin; SFN, sulforaphane; siRNA, small interfering RNA; TCA, tricarboxylic acid.

transcription of numerous hepatic genes associated with xenobiotic metabolism, detoxification, and clearance (Willson and Kliewer, 2002; Tolson and Wang, 2010). In addition to the well established role of PXR as a xenobiotic sensor, recent studies have extended the role of PXR to the regulation of various physiologic processes in control of energy homeostasis. For instance, activation of PXR is associated with upregulation of lipogenic enzymes such as stearoyl CoA desaturase 1, fatty acid elongase, peroxisome proliferator-activated receptor γ, and the fatty acid transporter CD36 (Zhou et al., 2008; Wada et al., 2009). PXR can also interact with the insulin response forkhead FoxA2 and indirectly affect fatty acid β-oxidation (Nakamura et al., 2007). In cultured mouse primary hepatocytes, activation of PXR by either ligand binding or post-translational modification resulted in significant lipid accumulation (Biswas et al., 2011; Staudinger et al., 2011). On the other hand, ablation of PXR alleviates high-fat diet–induced obesity, hepatic steatosis, and insulin resistance in mice (Biswas et al., 2009; He et al., 2013). Collectively, these results suggest that activation of PXR may not only influence genes involving xenobiotic metabolism/detoxification, but also functions as a metabolic sensor affecting energy metabolism associated with various metabolic disorders.

Accumulating evidence thus far reveals that many xenobiotics, including clinically used drugs, can induce hepatic steatosis as an early manifestation of liver toxicity (Farrell, 2002). Drugs, through their modulation of peroxisome proliferator-activated receptor, liver X receptor, farnesoid X receptor, as well as PXR and its sister receptor the constitutive androstane receptor, have been shown to affect liver fat metabolism and accumulation (Kalaany and Mangelsdorf, 2006; Kallwitz et al., 2008; Konno et al., 2008). Our recent microarray results indicated that the *SLC13A5* gene can be induced by rifampicin (RIF), the prototypical agonist of human PXR in human primary hepatocytes (HPH) (unpublished data). Thus, we hypothesize that inductive expression of SLC13A5 can be transcriptionally regulated by PXR, and perturbation of hepatic SLC13A5 expression may contribute to drug-induced hepatic steatosis.

In this report, we provide experimental evidence to show that the human *SLC13A5* gene is a novel transcriptional target of PXR, which can be upregulated in HPH through specific interaction of PXR with two enhancer modules located upstream of the *SLC13A5* promoter. Additionally, knockdown of SLC13A5 expression is associated with decreased lipid accumulation in human liver cells. Thus, our results reveal that PXR-mediated transcription of SLC13A5 may represent a novel mechanism contributing to drug-induced hepatic steatosis.

Materials and Methods

Chemicals and Biologic Reagents. RIF and sulforaphane (SFN) were purchased from Sigma-Aldrich (St. Louis, MO). Oligonucleotide primers were synthesized by Integrated DNA Technologies, Inc. (Coralville, IA). The Dual-Luciferase Reporter Assay System was purchased through Promega (Madison, WI). Antibodies against SLC13A5 and CYP3A4 were from Abcam (Cambridge, MA) and Millipore Corporation (Billerica, MA), respectively. β-Actin antibody was from Sigma-Aldrich. Matrigel, insulin, and ITS$^+$ (6.25 μg/ml insulin, 6.25 μg/ml transferrin, and 6.25 ng/ml selenium) were obtained from BD Biosciences (Bedford, MA). Other cell culture reagents were purchased from Life Technologies (Grand Island, NY) or Sigma-Aldrich.

Plasmid Construction and Mutagenesis. The pSG5–human PXR (hPXR) expression vector was obtained from Dr. Steven Kliewer (University of Texas Southwestern Medical Center, Dallas, TX). The SLC13A5 promoter region encompassing the sequence between +87 and −923 was polymerase chain reaction (PCR)–amplified using primers 5′-ACTAGCTAGC-GAAGAAAATCACAGAGG-3′ and 5′-ATA-TATGAAGCTTGCGCGGGAGGGAGAC-3′, and subsequently cloned into the NheI-HindIII sites of pGL3-basic vector generating reporter construct, namely, SLC13A5-1k. The two enhancer modules located at −22 and −1.7 kb upstream of SLC13A5 were amplified using primers 5′-CGGGCTAGCCTTCAGTCTCCACCCCAAGAT-3′, 5′-ATGTACCC-TGACTATGCCTTC-3′ and 5′-GAAGGCATAGTCAGGGTACATCAGACG-CGGTGGCTC-3′, 5′-CTAGCTAGCGCACGATCTCGGCTCACTGCA-3′ to generate the 274- and 239-bp PCR products, respectively. These two PCR products were cloned into the SLC13A5-1kb vector, creating a construct containing the SLC13A5 proximal promoter (1kb) and the distal elements, termed SLC13A5-1k/DR4-1/2. An 81-bp fragment containing three repeats of the distal DR4-1 element was cloned into the pGL3-TK plasmid, and termed SLC13A5-(DR4-1)3. Site-directed mutagenesis of the elements was carried out using the QuikChange site-directed mutagenesis kit (Stratagene, CA) according to the manufacturer's introduction. The following primers were used for mutagenesis: DR4-1mut (underlines indicate mutated bases), 5′-CTTTTCTATGGACTCATCCGAGCGCT-CCCCTTCTCCCCAGGC-3′; DR4-2mut, 5′-GGTGGGCGGATCACCT-GACCTGAGGAGTTCGAGACCAG -3′. All constructs were verified by sequencing. The pRL-TK *Renilla* luciferase plasmid used to normalize firefly luciferase activities was from Promega.

HPH Cultures and Treatments. Liver tissues were obtained by medical staff after donor consent and prior approval from the Institutional Review Board at the University of Maryland School of Medicine. Hepatocytes were isolated from human liver specimens by a modification of the two-step collagenase digestion method as described previously (Hamilton et al., 2001), or were obtained from Bioreclamation In Vitro Technologies (Baltimore, MD). Hepatocytes were seeded at 1.5×10^6 cells/well in six-well BioCoat plates (BD Biosciences) and cultured in the sandwich format as described previously (Faucette et al., 2007). HPH were maintained for 36 hours before treatment with 0.1% dimethylsulfoxide (DMSO), RIF (10 μM), or SFN (10 μM) for 24 or 72 hours for detection of mRNA and protein expression, respectively. For detailed concentration-response studies, hepatocytes were exposed for 24 hours to RIF (1–25 μM), whereas in time-response studies, cells were exposed to RIF (10 μM) for 2–48 hours. Culture medium was replaced on a daily basis.

Animals. Human PXR-transgenic mice with CB6F1 genetic background were established as previously described (Xie et al., 2000a). Mice were kept in 12/12-hour dark/light cycle and fed a standard solid diet ad libitum. hPXR-transgenic female mice received vehicle control (4% DMSO in saline) or RIF (20 mg/kg) daily via intraperitoneal injection for 5 days. Twenty-four hours after dosing, animal livers were harvested for further analysis. The use of mice in this study has complied with relevant federal guidelines and institutional policies.

Transfection in Hepatoma Cells and HPH. HepG2 cells cultured in 24-well plates were transfected with different *SLC13A5* reporter constructs (60 ng/well) in the presence of the hPXR expression vector using the Fugene 6 Transfection Kit (Roche, Indianapolis, IN) following the manufacturer's instruction. Twenty-four hours after transfection, cells were treated with vehicle control (0.1% DMSO) or RIF (10 μM) for another 24 hours. Subsequently, cell lysates were assayed for firefly activities normalized against the activities of cotransfected *Renilla* luciferase using the Dual-Luciferase Kit (Promega). To characterize the function of SLC13A5 on lipid accumulation, HepG2 cells were transfected with predesigned small interfering RNA (siRNA) specific for SLC13A5 (siRNA-SLC13A5, 100 nM) or the AllStars negative control siRNA (siRNA-NC, 100 nM) from Qiagen (Germantown, MD) using Lipofectamine 2000 transfection reagent (Life Technologies). Seventy-two hours after transfection, intracellular lipid droplets were subjected to boron-dipyrromethene (BODIPY) staining followed by fluorescence microscopy visualization. The fluorescence intensity of BODIPY was

quantified using the National Institutes of Health ImageJ software (Bethesda, MD). In separate experiments, HPH seeded in 24-well BioCoat plates were transfected with SLC13A5-(DR4-1)3 construct in the presence of pRL-TK vector using Effectene reagent (Qiagen) as described previously (Faucette et al., 2007). Transfected HPH were treated with 0.1% DMSO or RIF (10 μM) for 24 hours. Cell lysates were subjected to dual-luciferase analysis as described earlier.

Real-Time PCR Analysis. Total RNA was isolated using the RNeasy Mini Kit (Qiagen) and reverse transcribed using a High Capacity cDNA Archive Kit (Applied Biosystems, Foster City, CA) following the manufacturers' instructions. Real-time PCR assays were performed on an ABI Prism 7000 Sequence Detection System (Applied Biosystems). Primers for the human SLC13A5, CYP3A4, PXR, and glyceraldehyde-3-phosphate dehydrogenase (GAPDH) include: SLC13A5, 5'-CTTTGT-GGCCACCCTGCTATTC-3' and 5'-AGCAAATCCGCCCCCTAGTA-3'; CYP3A4, 5'-GTGGGGCTTTTATGATGGTCA-3' and 5'-GCCTCAGAT-TTCTCACCAACACA-3'; PXR, 5'-AAGCCCAGTGTCAACGCAG-3' and 5'-GGGTCTTCCGGGTGATCTC-3'; and GAPDH, 5'-CCCATCACC-ATCTTCCAGGAG-3' and 5'-GTTGTCATGGATGACCTTGGC-3', and their mouse counterparts include the following: Slc13a5, 5'-TCTGATA-CCTGACAAGTTTGCC-3'and 5'-GTCCAGAACCTTCAAAAGTGGG-3'; Cyp3a11, 5'-GTCAAACGCCTCTCCTTGCTG-3' and 5'- GGCTTGCCTTC-TTTGCCTTC-3'; and Gapdh, 5'-TCCACTCACGGCAAATTCAACG-3' and 5'-TAGACTCCACGACATACTCAGC-3'. Induction values were calculated according to the following equation: fold over control = $2^{\Delta\Delta Ct}$, where ΔCt represents the differences in cycle threshold numbers between the target gene and GAPDH, and $\Delta\Delta Ct$ represents the relative change in these differences between control and treatment groups.

Western Blot Analysis. Cell homogenate proteins were resolved on SDS–polyacrylamide gels (12%) and electrophoretically transferred onto blotting membranes. Subsequently, membranes were incubated with antibodies against SLC13A5 (diluted 1:200), CYP3A4 (diluted 1:5000), or β-actin (Sigma-Aldrich). Blots were washed and incubated with horseradish peroxidase secondary antibodies, and developed using enhanced chemiluminescence Western blotting detection reagent from GE Healthcare (Pittsburgh, PA).

Electrophoretic Mobility Shift Assays. Electrophoretic mobility shift assay (EMSA) was carried out as described previously (Honkakoski et al., 1998). DNA probes were labeled with [α-^{32}P]dATP and nuclear receptor proteins were synthesized using the TNT quick-coupled in vitro transcription/translation system (Promega). A typical binding reaction (10 μl) contains 10 mM HEPES (pH 7.6), 0.5 mM dithiothreitol, 15% glycerol, 0.05% NP40, 50 mM NaCl, 2 μg of poly(dI-dC), 1 μl of in vitro translated proteins, and 4×10^4 cpm of labeled probe. Reaction mixtures were resolved on 5% acrylamide gels and ran in 45 mM Tris–boric acid buffer containing 1 mM EDTA at 150 V for 2 hours. Subsequently, gels were dried under vacuum and subjected to autoradiography at $-70°C$.

Chromatin Immunoprecipitation Assays. Treated HPH were cross-linked and processed using a chromatin immunoprecipitation (ChIP) assay kit (Millipore Corporation) according to the manufacturer's instruction. Precleared chromatin solutions were incubated with 3 μg of anti-PXR antibody (Santa Cruz Biotechnology, Dallas, TX) or normal rabbit IgG at 4°C overnight, from which immunoprecipitated samples were collected to purify DNA using the QIAquick PCR purification kit (Qiagen). Quantitative PCR was performed as previously mentioned using the following primers: SLC13A5-DR4-1, 5'-CTTCAGTCTCCACCCCAA-GAT-3' and 5'-ATGTACCCTGACTATGCCTTC-3'; SLC13A5-DR4-2, 5'-ATTTGGGCCAGACGCGGTGGCTC-3' and 5'-GCACGATCTCGGC-TCACTGCA-3'.

PXR Knockdown in HPH. Twenty-four hours after seeding, HPH were infected for 4 hours with negative control or small hairpin RNA against hPXR lentiviral particles that were packaged in human embryonic kidney 293T cells using the MISSION Lentiviral Packaging Mix System (Sigma-Aldrich). Infected hepatocytes were cultured in serum-free Williams' E medium for 48 hours before treatment with 0.1% DMSO or RIF (10 μM) for 24 hours. Total RNA was prepared for real-time PCR analysis as described earlier.

Oil Red O/BODIPY Staining Assays. HPH were pretreated with 0.1% DMSO or RIF (10 μM) for 72 hours before being cotreated with oleate acid conjugated with 5% bovine serum albumin prepared as described elsewhere for another 24 hours (Mei et al., 2011). Treated hepatocytes were fixed with formaldehyde, then stained with Oil Red O for 1 hour at room temperature. Adipose conversion was quantitated using a spectrophotometer as described previously (Ramirez-Zacarias et al., 1992). Cellular lipid droplets were visualized under fluorescence microscopy after BODIPY staining.

Statistical Analysis. All data represent at least three independent experiments and were expressed as the mean $\pm$ S.D. Statistical comparisons were made using one-way analysis of variance followed by a post-hoc Dunnett's test or Student's t test where appropriate. Statistical significance was set at $P < 0.05$ and $P < 0.01$.

Results

RIF Induces Expression of the SLC13A5 Gene in HPH. As shown in Fig. 1, mRNA expression of SLC13A5 was increased by RIF in a concentration- and time-dependent manner, reaching plateaus at 10 μM and around 24 hours after treatment, respectively (Fig. 1, A and B). At the concentration typically used for PXR activation, RIF (10 μM) robustly induced SLC13A5 mRNA by 12- to 27-fold in HPH prepared from multiple liver donors (Fig. 1C). Induction of SLC13A5 protein was also observed upon RIF treatment in HPH from the same panel of donors (Fig. 1E). As expected, CYP3A4, the prototypical target gene of PXR, was also induced by RIF (Fig. 1, D and E). These results suggest that the *SLC13A5* gene is highly inducible in RIF-treated HPH; PXR is most likely the transcription factor that mediates the induction of this citrate uptake transporter in human liver.

Inhibition of PXR Affects Drug-Induced SLC13A5 Expression. To further correlate contribution of PXR in the induction of SLC13A5 expression, HPH were treated with RIF in the presence or absence of SFN, a selective PXR deactivator (Zhou et al., 2007). Clearly, RIF-induced expression of SLC13A5 and CYP3A4 was significantly suppressed by SFN (Fig. 2A). In separate experiments, knockdown of human PXR expression by lentiviral–small hairpin RNA markedly attenuated RIF-mediated induction of SLC13A5 and CYP3A4 without affecting their basal expression in HPH (Fig. 2, B–D). Next, we extended our investigation to an in vivo environment, where humanized PXR–transgenic mice were treated with RIF, the selective human PXR activator, as outlined in *Materials and Methods*. Expression of the *Slc13a5* gene was significantly induced by the activation of hPXR in the transgenic mice (Fig. 2E). Together, these results strongly support that SLC13A5 is a transcriptional target of human PXR.

Identification of PXR-Response Elements in the Upstream of SLC13A5 Gene. To delineate the molecular mechanism(s) by which PXR regulates *SLC13A5* gene expression, we initially carried out in silico analysis of up to -30 kb of the upstream sequence of *SLC13A5* gene using the NUBIScan version 2.0 (http://www.nubiscan.unibas.ch/). Two clusters of potential PXR binding sites were identified at approximately -1.7 and -22 kb with response motifs exhibiting high sequence homology to the consensus core site of AGGTCA spaced by 4 nucleotides (DR4). As shown in Fig. 3A, three DR4 motifs in the two clusters were designated as DR4-1, DR4-2 and DR4-3. Utilizing in vitro EMSA, we found that heterodimer of PXR and the retinoid X receptor binds specifically to DR4-1 and DR4-2 at intensities equal to or exceeding that of the everted-repeat (ER6) element
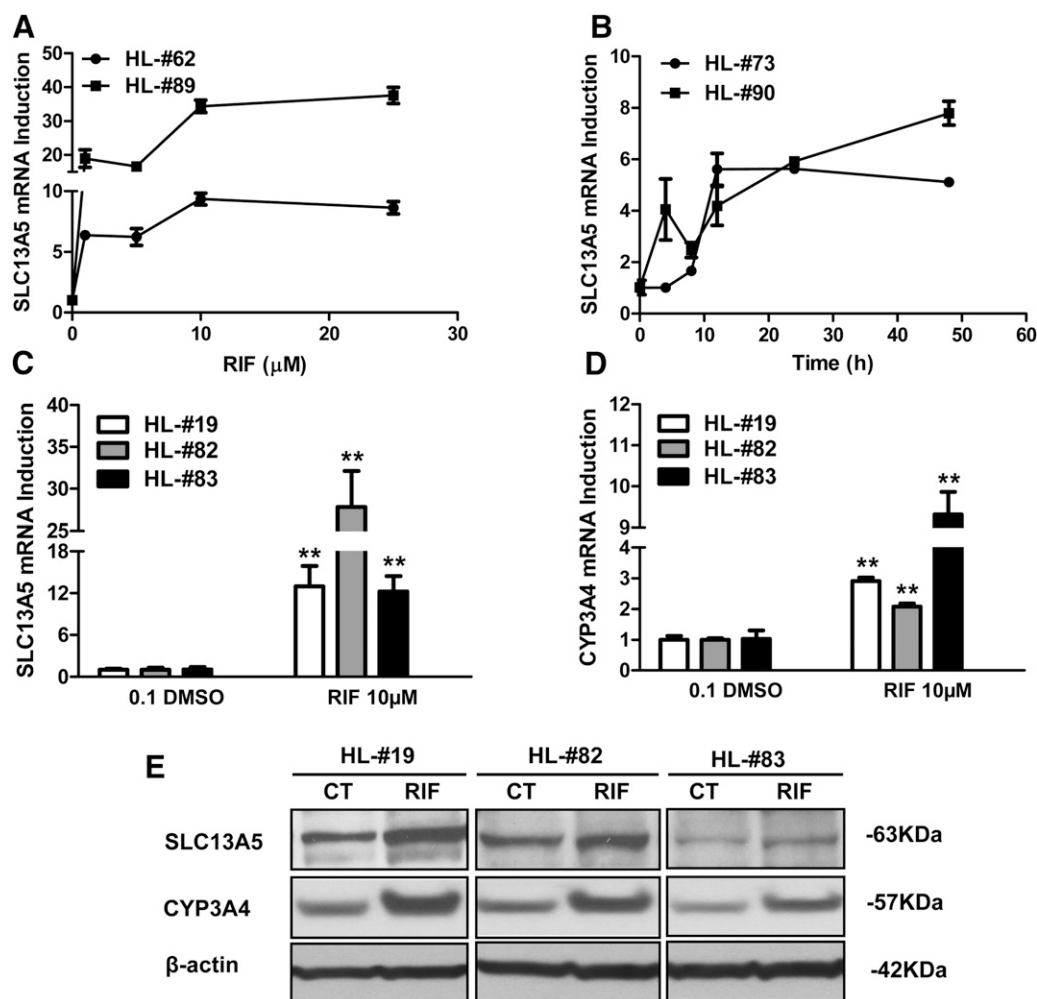
Fig. 1. Induction of SLC13A5 by PXR activation. HPH prepared from two liver donors were treated with RIF at multiple concentrations (HL62 and 89) for 24 hours (A) or at different time points (HL73 and 90) (B). Concentration- and time-dependent induction of SLC13A5 mRNA was detected using real-time PCR as outlined in *Materials and Methods*. In separate experiments, HPH from liver donors (HL19, 82, and 83) were treated with 0.1% DMSO or RIF (10 μM) for 24 or 72 hours analyze mRNA and protein, respectively. Expression of SLC13A5 mRNA (C), CYP3A4 mRNA (D), and their proteins (E) was measured using real-time PCR and Western blotting assays. Results are expressed as the mean $\pm$ S.D. (n = 3). **$P < 0.01$. CT, control (0.1% DMSO).

from *CYP3A4* promoter (Fig. 3B). Competition assays revealed that these bindings can be efficiently blocked by unlabeled DR4-1, DR4-2, or CYP3A4/ER6, but not by their respective mutants (Fig. 3C). Comparatively, DR4-1 exhibited stronger binding to PXR than DR4-2.

Furthermore, to demonstrate in vivo recruitment of PXR to the DR4-1– and DR4-2–containing regions of SLC13A5, ChIP assays were performed in HPH from two liver donors (HL98 and 99). As shown in Fig. 3, D and E, RIF treatment resulted in the recruitment of PXR to the ER6-containing region from CYP3A4 and the DR4-1–containing module of SLC13A5. On the other hand, it is interesting to note that, in contrast to the chemical-mediated recruitment of PXR to the DR4-1 region and results from EMSA, PXR failed to interact with the DR4-2 region in HPH regardless of RIF stimulation (Fig. 3E).

Activation of PXR Increases SLC13A5 Report Activity in HepG2 and HPH. To characterize the functional relevance of the PXR-binding elements in SLC13A5 transactivation, a number of *SLC13A5* promoter constructs have been generated as depicted in Fig. 4. In HepG2 cells cotransfected with the SLC13A5-1k/DR4-1/2 luciferase and different amounts of hPXR expression vectors, corresponding luciferase activities were

increased along with increasing amounts of PXR plasmid, and RIF significantly enhanced the SLC13A5 luciferase activity when PXR was cotransfected at quantities of 30 and 60 ng (Fig. 4A). In site-directed mutagenesis experiments, RIF-mediated transactivation of SLC13A5-luciferase activity through PXR was clearly abrogated by the mutation of DR4-1 but only moderately affected by the DR4-2 mutation (Fig. 4B). Additionally, we showed that the construct containing three-repeat of the distal DR4-1 exhibits stronger activation stimulated by RIF in both HepG2 cells with the cotransfection of PXR and HPH expressing endogenous PXR (Fig. 4, C and D). These data further emphasize the role of the two enhancer modules, particularly DR4-1, in PXR-mediated transactivation of SLC13A5.

RIF Increases Lipid Accumulation in HPH. By activating PXR, RIF changes the expression of many genes potentially associated with energy homeostasis, including SLC13A5, as observed in this study. To examine the steatogenic potential of PXR, HPH from two donors (HL66 and 70) were treated with RIF for 72 hours prior to loading of oleate, as described in *Materials and Methods*. Quantitative analysis of the Oil Red staining demonstrated that RIF significantly increased lipid
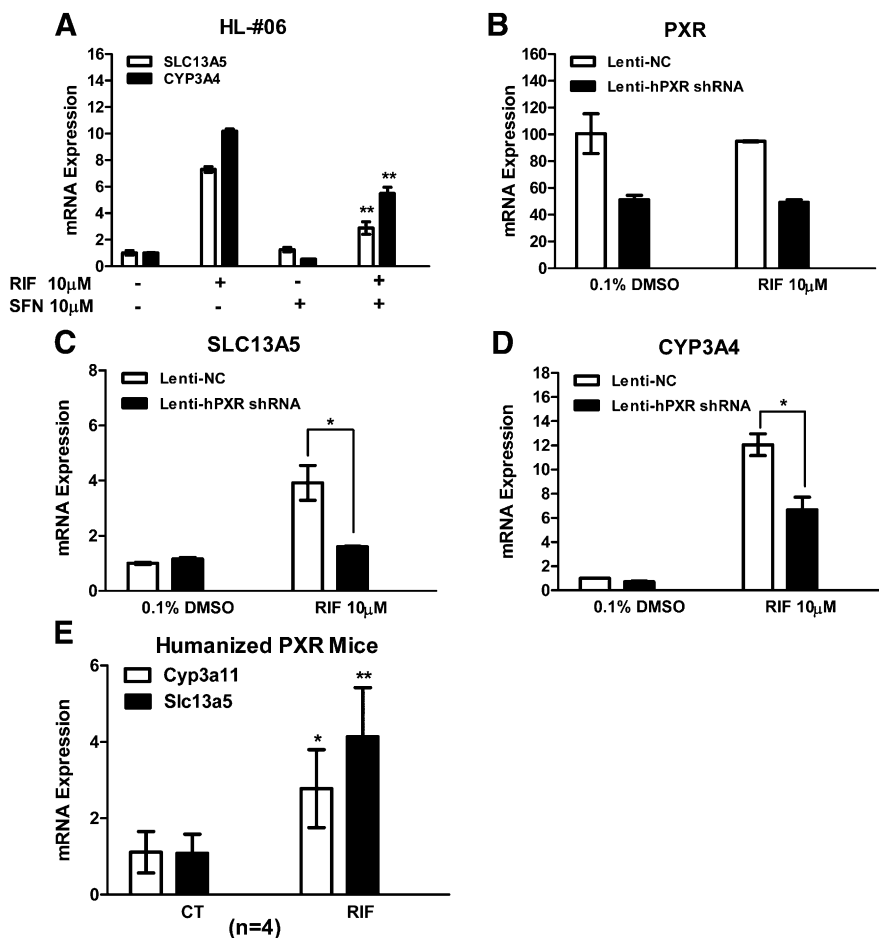
Fig. 2. Influence of PXR expression and activity on the induction of SLC13A5. HPH from a liver donor (HL06) were treated with 0.1% DMSO, RIF (10 μM), SFN (10 μM) alone, or cotreatment of SFN with RIF (A). Twenty-four hours after treatment, total RNA was isolated and reverse transcribed for real-time PCR analysis of SLC13A5 and CYP3A4 expression. HPH (HL71) were infected with lentiviral-hPXR–small hairpin RNA or lentiviral–negative control (Lenti-NC) followed by the treatment of 0.1% DMSO or RIF (10 μM) as detailed in *Materials and Methods*. Expression of PXR (B), SLC13A5 (C), and CYP3A4 (D) was measured by real-time PCR. In separate experiments, hPXR-transgenic mice were given vehicle control (4% DMSO in saline) or RIF (20 mg/kg) as detailed in *Materials and Methods*. Real-time PCR was used to measure the relative mRNA amount of Cyp3a11 and Slc13a5 genes (E). Data are expressed as the mean $\pm$ S.D. (n = 3 for HPH treatment; n = 4 for animal study). *$P < 0.05$; **$P < 0.01$. CT, vehicle control.

accumulation in HPH (Fig. 5A). This enhancement was also visualized under fluorescence microscopy with cellular lipids stained by BODIPY (Fig. 5B).

Knockdown of SLC13A5 Expression Decreases Lipid Formation in HepG2 Cells. Finally, we tested whether knockdown of SLC13A5 alone is associated with decreased lipid accumulation in HepG2 cells which maintain a relatively high level of endogenous SLC13A5 expression. As shown in Fig. 6A, expression of both mRNA and protein of SLC13A5 was significantly repressed 72 hours after transfection of siRNA-SLC13A5. BODIPY staining of the transfected cells revealed that lipid content was significantly decreased in HepG2 cells with decreased SLC13A5 expression (Fig. 6B). These data indicate that knockdown of SLC13A5 is sufficient to repress lipid formation in HepG2 cells, suggesting that perturbation of SLC13A5 may contribute to drug-induced steatotic response.

Discussion

SLC13A5, the sodium-coupled citrate transporter, represents the rate-limiting machinery governing the influx of citrate from circulation to the liver cells, where it plays critical roles in fatty acid synthesis, cholesterol synthesis, glycolysis, and gluconeogenesis (Inoue et al., 2002c, 2004). The potential importance of SLC13A5 in energy homeostasis has been heightened in a recent publication (Birkenfeld et al., 2011). Nevertheless, how the *SLC13A5* gene is transcriptionally regulated and whether clinically used drugs could disturb the expression of this transporter

are largely unknown. In this study, we have shown that *SLC13A5* is a novel target of PXR, and transcription of *SLC13A5* was robustly induced by RIF (a selective activator of human PXR) in HPH. We have also identified and functionally characterized two enhancer modules located upstream of the *SLC13A5* gene that are associated with regulation of PXR-mediated induction of SLC13A5. Moreover, our data reveal that SLC13A5 induction was positively correlated with RIF-mediated fat accumulation in HPH, whereas knockdown of SLC13A5 significantly decreased lipid content in HepG2 cells.

As the newest member identified in the sodium dicarboxylate cotransporter family, SLC13A5 is predominantly expressed in the liver, with moderate levels in the brain and testes (Inoue et al., 2002b,c). To date, knowledge regarding the molecular control of *SLC13A5* gene expression is limited. It was reported previously that the activity of SLC13A5 was significantly stimulated by therapeutic concentrations of lithium, with enhanced substrate affinity, but without affecting its expression (Inoue et al., 2003). Recently, two genome-wide DNA methylation studies revealed that SLC13A5 expression in glioblastoma and renal cancer cells was inversely associated with DNA hypermethylation in the promoter of SLC13A5, indicating that this gene might be epigenetically regulated under certain disease conditions (Etcheverry et al., 2010; Arai et al., 2012). Our results are the first to show that *SLC13A5* is a highly inducible gene associated with chemical-stimulated activation of PXR in human liver. It is well known that, as a xenobiotic sensor, PXR stimulates gene expression by
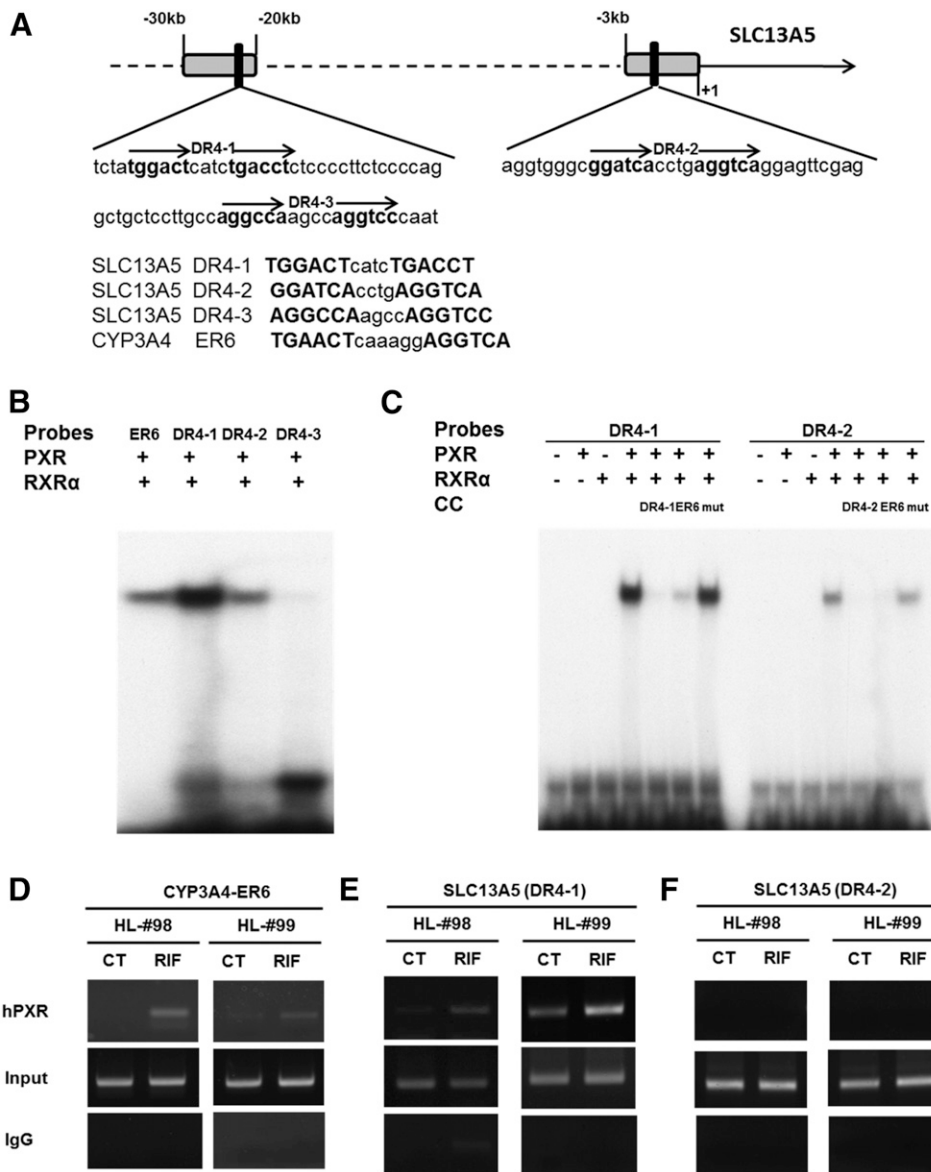
A

DR4-1
tctat**tggact**catc**tgacct**ctcccccttctccccag

DR4-2
aggtgggc**ggatca**cctg**aggtca**ggagttcgag

DR4-3
gctgctccttgcc**aggcca**agcc**aggtcc**caat

SLC13A5 DR4-1   **TGGACT**catc**TGACCT**
SLC13A5 DR4-2   **GGATCA**cctg**AGGTCA**
SLC13A5 DR4-3   **AGGCCA**agcc**AGGTCC**
CYP3A4 ER6   **TGAACT**caaagg**AGGTCA**

B

Probes	ER6	DR4-1	DR4-2	DR4-3
PXR	+	+	+	+
RXRα	+	+	+	+

C

Probes	DR4-1						DR4-2					
PXR	-	+	-	+	+	+	-	+	-	+	+	+
RXRα	-	-	+	+	+	+	-	-	+	+	+	+
CC					DR4-1	ER6 mut					DR4-2	ER6 mut

D CYP3A4-ER6

	HL-#98		HL-#99	
	CT	RIF	CT	RIF
hPXR				
Input				
IgG				

E SLC13A5 (DR4-1)

	HL-#98		HL-#99	
	CT	RIF	CT	RIF
hPXR				
Input				
IgG				

F SLC13A5 (DR4-2)

	HL-#98		HL-#99	
	CT	RIF	CT	RIF
hPXR				
Input				
IgG				

Fig. 3. Binding of PXR to enhancers identified upstream of SLC13A5 promoter. A computer-based search of −30 kb of SLC13A5 upstream resulted in the identification of PXR-responsive elements located at −22 and −1.7 kb (A). In vitro binding of the predicted DR4 elements with PXR/retinoid X receptor α (RXRα) heterodimer was measured using electrophoretic mobility shift assays (B and C). Oligonucleotide probes were labeled with [α-^{32}P]dATP. Unlabeled oligonucleotides were used as cold competitor (CC). HPH from liver donors (HL98 and 99) were treated with 0.1% DMSO or RIF (10 μM). As detailed in *Materials and Methods*, ChIP assays were used to analyze drug-induced recruitment of PXR to the CYP3A4/ER6 (D) and DR4-1 and DR4-2 containing regions of SLC13A5 (E and F). After precipitation with IgG or PXR antibody, related ER6, DR4-1, and DR4-2 regions were amplified by PCR. CT, control (0.1% DMSO).

binding to consensus xenobiotic response elements located in its target gene promoters (Xie et al., 2000b; Wang and LeCluyse, 2003). After computational analysis of the −30-kb upstream region of the *SLC13A5* gene, two PXR response elements at −22 and −1.7 kb were identified containing DR4 motifs, with the distal DR4-1 having the most sequence homology to the distal enhancer module of CYP3A4. In vitro EMSA demonstrated that the DR4-1 exhibited binding capacity to PXR/retinoid X receptor α heterodimer equal to or greater than that of the CYP3A4/ER6. In characterizing the recruitment of PXR to the DR4-1– and DR4-2–containing regions in a physiologically relevant system, results from our ChIP assays in HPH showed that RIF has clearly enhanced the interaction of DR4-1 with PXR. In contrast, the DR4-2–containing region appears not to be associated with PXR in HPH. Although we are not able to explain this later phenomenon entirely, the DR4-2 element might be less important regarding xenobiotics-induced expression of SLC13A5. However, it is not uncommon that regulatory elements in the promoter of mammalian genes are spread remotely, encompassing a long scale of DNA sequence (Hagege et al., 2007). In fact,

a number of PXR target genes contain functional distal response elements located upstream of their promoters, including *CYP3A4, CYP2B6,* and *MDR1* (Goodwin et al., 1999; Geick et al., 2001; Wang et al., 2003).

Insertion of a 247- and 239-bp fragment containing the DR4-1 and DR4-2 element, respectively, in the SLC13A5-1kb promoter has resulted in PXR-dependent activation in HepG2 cells. Notably, mutation of DR4-1 completely abolished its response to PXR, whereas DR4-2 mutant only exhibited a moderate decrease in PXR-based activation. Consistent with the binding assays, these results again demonstrate that the distal DR4-1 is critical in chemical-mediated induction of SLC13A5. Of importance, our results showed that physiologically relevant expression of endogenous nuclear receptors in HPH was able to activate the *SLC13A5* promoter upon RIF treatment.

SLC13A5 is the mammalian ortholog of the "I'm not dead yet" (*Indy*) gene in *Drosophila melanogaster* (Inoue et al., 2002a). Reduced expression of *Indy* and its homologs has been established as a critical determinant of extending life span in
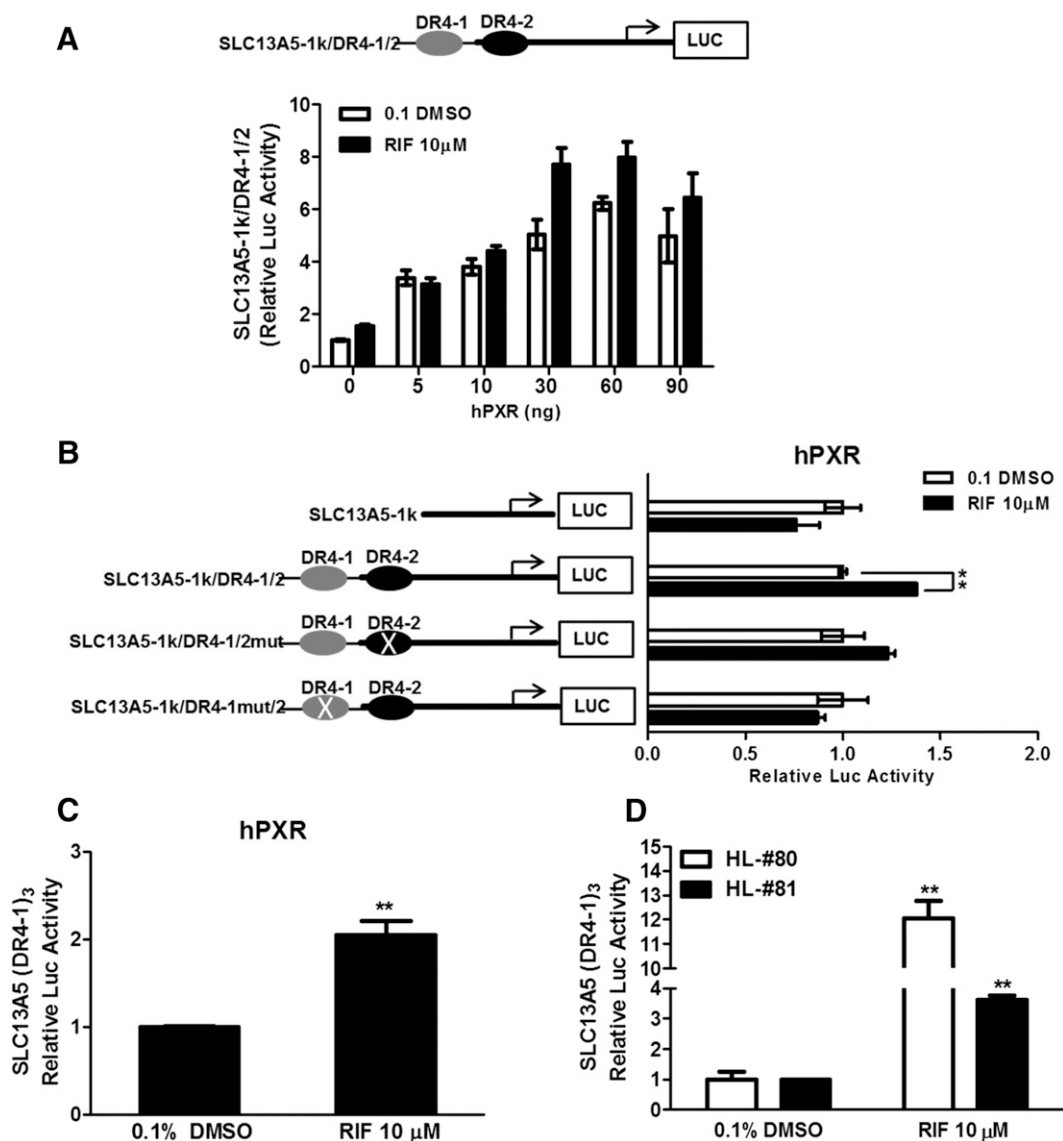
Fig. 4. Activation of the *SLC13A5* promoter by human PXR. HepG2 cells were cotransfected with SLC13A5-1k/DR4-1/2 in the presence of different amounts of hPXR expression vector (A), cotransfected with the wild-type/mutant *SLC13A5* promoter constructs (B) or the SLC13A5-(DR4-1)3 (C) with PXR for 24 hours. In separate experiments, SLC13A5-(DR4-1)3 was transfected in HPH (HL80 and 81) without exogenous expression of PXR (D). Subsequently, all transfected cells were treated with 0.1% DMSO or RIF (10 μM) for 24 hours. Luciferase activities were measured using the Dual-Luciferase reagent (Promega) in cell extracts according to the manufacturer's instructions. Three independent measures from each treatment were analyzed. **$P < 0.01$. LUC, luciferase.

this organism mimicking calorie restriction (Knauf et al., 2006). Given the importance of citrate in fatty acid synthesis and energy metabolism, it is reasonable to postulate that perturbation of SLC13A5 expression and/or function would influence hepatic fat accumulation and related metabolic syndromes. In line with this premise, Inoue et al. (2003) showed that lithium stimulation significantly increased SLC13A5-dependent [^{14}C]citrate uptake and incorporation into lipids in HepG2 cells. Most recently, utilizing *Slc13a5* knockout mice, Birkenfeld et al. (2011) demonstrated that mice lacking Slc13a5 expression were protected from high-fat diet–induced obesity and insulin resistance; in particular, deletion of Slc13a5 prevents lipid accumulation in the liver. In the current study, we showed that, as a potent inducer of SLC13A5, RIF enhances lipid accumulation in HPH. These results are in agreement with a previous report, in that by screening the steatogenic potential of 76 different nuclear receptor ligands, 18% of the examined ligands,

including RIF, exhibited enhanced lipid accumulation in human liver cells (Moya et al., 2010). On the other hand, ketoconazole, an established inhibitor of PXR, improved the metabolic function of high-fat diet–fed mice (Huang et al., 2007; He et al., 2013). Although activation of PXR may influence the expression of multiple genes associated with lipid metabolism such as CD36, stearoyl CoA desaturase 1, and long-chain fatty acid elongase, identification of SLC13A5 as a novel target gene of PXR further highlights the multifaceted role of this receptor in energy homeostasis. The correlation between SLC13A5 and fat accumulation was further supported by our observation that knockdown of SLC13A5 expression alone decreased lipid accumulation in HepG2 cells.

In summary, we demonstrate that *SLC13A5* is a highly inducible gene in human liver, and induction of this transporter is transcriptionally regulated by PXR. We have identified and characterized two distal responsive elements that are
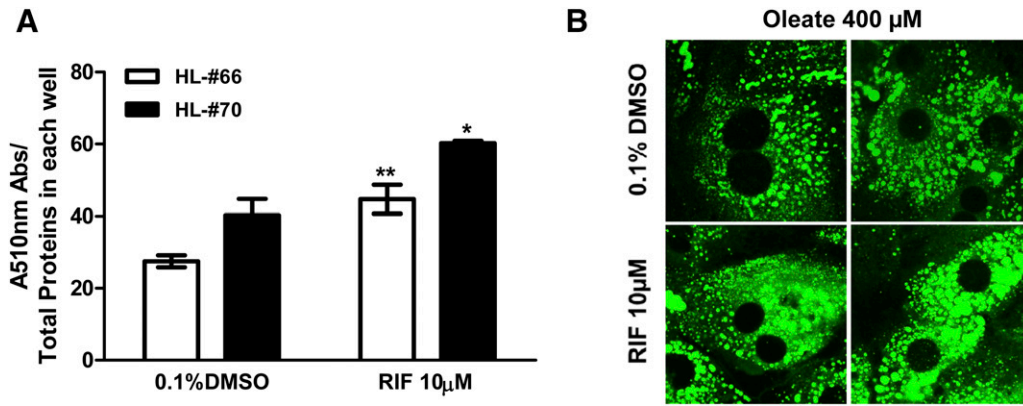
Fig. 5. RIF induces lipid accumulation in HPH. HPH from liver donors (HL66 and 70) were treated with 0.1% DMSO or RIF (10 μM) for 72 hours, before the cotreatment with oleate acid conjugated with 5% bovine serum albumin for another 24 hours. Lipid contents in treated cells were quantified by Oil Red O staining (A) or visualized under fluorescence microscopy by BODIPY staining (B) as detailed in *Materials and Methods*. Oil Red O quantifications were expressed as the mean $\pm$ S.D. (n = 3). *P < 0.05; **P < 0.01.

involved in PXR-mediated transactivation of the *SLC13A5* gene in human hepatocytes. Meanwhile, we do recognize that, in contrast to the potent induction of the SLC13A5 mRNA observed in HPH, activation of the SLC13A5 reporter construct by RIF is relatively moderate. This discrepancy may suggest that additional unidentified PXR response module (s) may exist, which warrants further extensive investigation. Overall, the present work further expands the role of PXR
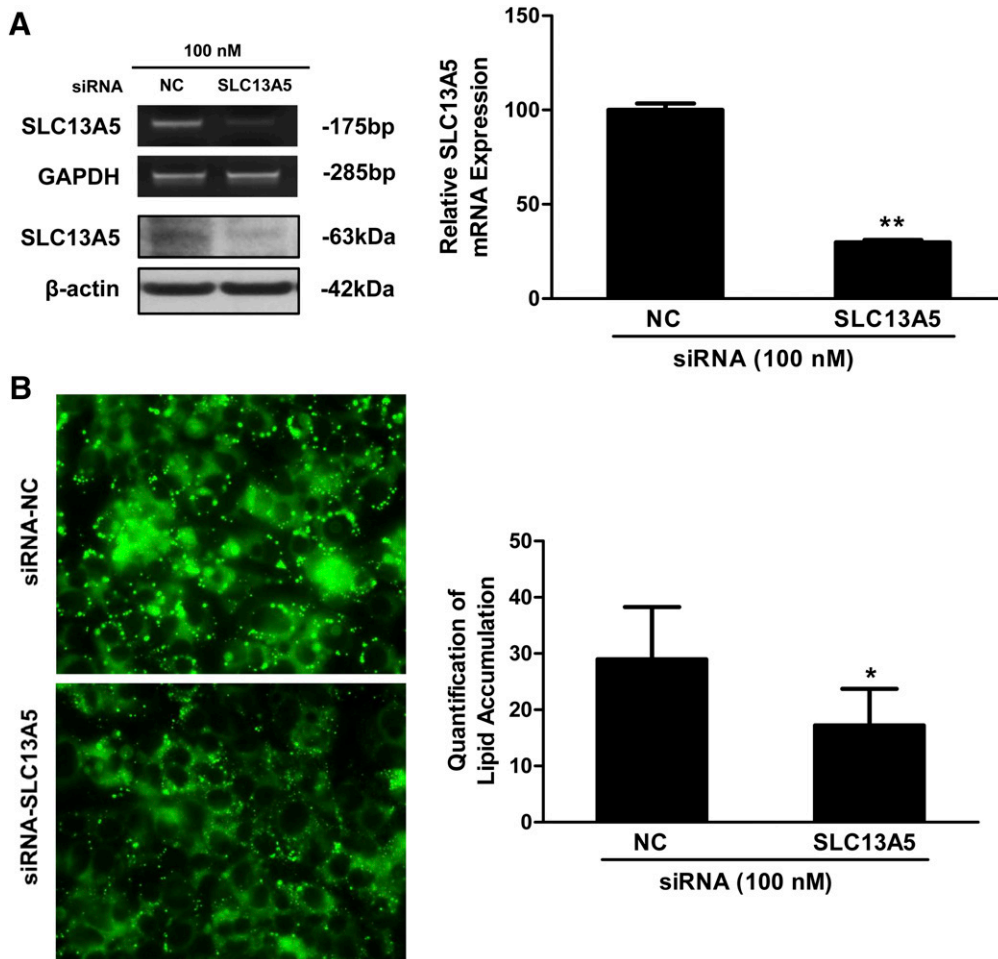

Fig. 6. Knockdown of SLC13A5 expression decreases lipid formation in HepG2 cells. HepG2 cells were transfected with siRNA-SLC13A5 or siRNA–negative control (NC) using Lipofectamine 2000 reagent. Seventy-two hours after transfection, intracellular lipid droplets were subjected to BODIPY staining and fluorescence microscopy visualization as outlined in *Materials and Methods*. Expression of SLC13A5 mRNA and protein was analyzed using real-time PCR and Western blotting (A). BODIPY staining of lipid contents was visualized and signal density quantified using National Institutes of Health ImageJ (B). Mean $\pm$ S.D. represents results from three independent experiments. *P < 0.05; **P < 0.01.

from xenobiotic metabolism/detoxification to energy metabolism and citrate biology. Furthermore, SLC13A5 may represent a novel therapeutic target for obesity and metabolic disorders.

Authorship Contributions

Participated in research design: L. Li, Xie, Sueyoshi, Negishi, Wang.

Conducted experiments: L. Li, H. Li, Garzel, Yang, Q. Li, Hu, Sueyoshi.

Contributed new reagents or analytic tools: Heyward, Moeller, Zhang, Shu.

Performed data analysis: L. Li, Wang.

Wrote or contributed to the writing of the manuscript: L. Li, Garzel, Xie, Sueyoshi, Negishi, Wang.

References

Arai E, Chiku S, Mori T, Gotoh M, Nakagawa T, Fujimoto H, and Kanai Y (2012) Single-CpG-resolution methylome analysis identifies clinicopathologically aggressive CpG island methylator phenotype clear cell renal cell carcinomas. *Carcinogenesis* **33**:1487–1493.

Birkenfeld AL, Lee HY, Guebre-Egziabher F, Alves TC, Jurczak MJ, Jornayvaz FR, Zhang D, Hsiao JJ, Martin-Montalvo A, and Fischer-Rosinsky A et al. (2011) Deletion of the mammalian INDY homolog mimics aspects of dietary restriction and protects against adiposity and insulin resistance in mice. *Cell Metab* **14**:184–195.

Biswas A, Mani S, Redinbo MR, Krasowski MD, Li H, and Ekins S (2009) Elucidating the 'Jekyll and Hyde' nature of PXR: the case for discovering antagonists or allosteric antagonists. *Pharm Res* **26**:1807–1815.

Biswas A, Pasquel D, Tyagi RK, and Mani S (2011) Acetylation of pregnane X receptor protein determines selective function independent of ligand activation. *Biochem Biophys Res Commun* **406**:371–376.

Chen XZ, Shayakul C, Berger UV, Tian W, and Hediger MA (1998) Characterization of a rat Na+-dicarboxylate cotransporter. *J Biol Chem* **273**:20972–20981.

Etcheverry A, Aubry M, de Tayrac M, Vauleon E, Boniface R, Guenot F, Saikali S, Hamlat A, Riffaud L, and Menei P et al. (2010) DNA methylation in glioblastoma: impact on gene expression and clinical outcome. *BMC Genomics* **11**:701.

Farrell GC (2002) Drugs and steatohepatitis. *Semin Liver Dis* **22**:185–194.

Faucette SR, Zhang TC, Moore R, Sueyoshi T, Omiecinski CJ, LeCluyse EL, Negishi M, and Wang H (2007) Relative activation of human pregnane X receptor versus constitutive androstane receptor defines distinct classes of CYP2B6 and CYP3A4 inducers. *J Pharmacol Exp Ther* **320**:72–80.

Geick A, Eichelbaum M, and Burk O (2001) Nuclear receptor response elements mediate induction of intestinal MDR1 by rifampin. *J Biol Chem* **276**:14581–14587.

Goodwin B, Hodgson E, and Liddle C (1999) The orphan human pregnane X receptor mediates the transcriptional activation of CYP3A4 by rifampicin through a distal enhancer module. *Mol Pharmacol* **56**:1329–1339.

Gopal E, Miyauchi S, Martin PM, Ananth S, Srinivas SR, Smith SB, Prasad PD, and Ganapathy V (2007) Expression and functional features of NaCT, a sodium-coupled citrate transporter, in human and rat livers and cell lines. *Am J Physiol Gastrointest Liver Physiol* **292**:G402–G408.

Hagège H, Klous P, Braem C, Splinter E, Dekker J, Cathala G, de Laat W, and Forné T (2007) Quantitative analysis of chromosome conformation capture assays (3C-qPCR). *Nat Protoc* **2**:1722–1733.

Hamilton GA, Jolley SL, Gilbert D, Coon DJ, Barros S, and LeCluyse EL (2001) Regulation of cell morphology and cytochrome P450 expression in human hepatocytes by extracellular matrix and cell-cell interactions. *Cell Tissue Res* **306**:85–99.

He J, Gao J, Xu M, Ren S, Stefanovic-Racic M, O'Doherty RM, and Xie W (2013) PXR ablation alleviates diet-induced and genetic obesity and insulin resistance in mice. *Diabetes* **62**:1876–1887.

Honkakoski P, Zelko I, Sueyoshi T, and Negishi M (1998) The nuclear orphan receptor CAR-retinoid X receptor heterodimer activates the phenobarbital-responsive enhancer module of the CYP2B gene. *Mol Cell Biol* **18**:5652–5658.

Huang H, Wang H, Sinz M, Zoeckler M, Staudinger J, Redinbo MR, Teotico DG, Locker J, Kalpana GV, and Mani S (2007) Inhibition of drug metabolism by blocking the activation of nuclear receptors by ketoconazole. *Oncogene* **26**:258–268.

Inoue K, Fei YJ, Huang W, Zhuang L, Chen Z, and Ganapathy V (2002a) Functional identity of Drosophila melanogaster Indy as a cation-independent, electroneutral transporter for tricarboxylic acid-cycle intermediates. *Biochem J* **367**:313–319.

Inoue K, Fei YJ, Zhuang L, Gopal E, Miyauchi S, and Ganapathy V (2004) Functional features and genomic organization of mouse NaCT, a sodium-coupled transporter for tricarboxylic acid cycle intermediates. *Biochem J* **378**:949–957.

Inoue K, Zhuang L, and Ganapathy V (2002b) Human Na+ -coupled citrate transporter: primary structure, genomic organization, and transport function. *Biochem Biophys Res Commun* **299**:465–471.

Inoue K, Zhuang L, Maddox DM, Smith SB, and Ganapathy V (2002c) Structure, function, and expression pattern of a novel sodium-coupled citrate transporter (NaCT) cloned from mammalian brain. *J Biol Chem* **277**:39469–39476.

Inoue K, Zhuang L, Maddox DM, Smith SB, and Ganapathy V (2003) Human sodium-coupled citrate transporter, the orthologue of Drosophila Indy, as a novel target for lithium action. *Biochem J* **374**:21–26.

Kalaany NY and Mangelsdorf DJ (2006) LXRS and FXR: the yin and yang of cholesterol and fat metabolism. *Annu Rev Physiol* **68**:159–191.

Kallwitz ER, McLachlan A, and Cotler SJ (2008) Role of peroxisome proliferators-activated receptors in the pathogenesis and treatment of nonalcoholic fatty liver disease. *World J Gastroenterol* **14**:22–28.

Knauf F, Mohebbi N, Teichert C, Herold D, Rogina B, Helfand S, Gollasch M, Luft FC, and Aronson PS (2006) The life-extending gene Indy encodes an exchanger for Krebs-cycle intermediates. *Biochem J* **397**:25–29.

Konno Y, Negishi M, and Kodama S (2008) The roles of nuclear receptors CAR and PXR in hepatic energy metabolism. *Drug Metab Pharmacokinet* **23**:8–13.

Mei S, Ni HM, Manley S, Bockus A, Kassel KM, Luyendyk JP, Copple BL, and Ding WX (2011) Differential roles of unsaturated and saturated fatty acids on autophagy and apoptosis in hepatocytes. *J Pharmacol Exp Ther* **339**:487–498.

Moya M, Gómez-Lechón MJ, Castell JV, and Jover R (2010) Enhanced steatosis by nuclear receptor ligands: a study in cultured human hepatocytes and hepatoma cells with a characterized nuclear receptor expression profile. *Chem Biol Interact* **184**:376–387.

Nakamura K, Moore R, Negishi M, and Sueyoshi T (2007) Nuclear pregnane X receptor cross-talk with FoxA2 to mediate drug-induced regulation of lipid metabolism in fasting mouse liver. *J Biol Chem* **282**:9768–9776.

Pajor AM (1995) Sequence and functional characterization of a renal sodium/dicarboxylate cotransporter. *J Biol Chem* **270**:5779–5785.

Pajor AM (2014) Sodium-coupled dicarboxylate and citrate transporters from the SLC13 family. *Pflugers Arch* **466**:119–130.

Raimundo N, Baysal BE, and Shadel GS (2011) Revisiting the TCA cycle: signaling to tumor formation. *Trends Mol Med* **17**:641–649.

Ramírez-Zacarías JL, Castro-Muñozledo F, and Kuri-Harcuch W (1992) Quantitation of adipose conversion and triglycerides by staining intracytoplasmic lipids with Oil red O. *Histochemistry* **97**:493–497.

Staudinger JL, Xu C, Biswas A, and Mani S (2011) Post-translational modification of pregnane x receptor. *Pharmacol Res* **64**:4–10.

Stobbe MD, Houten SM, van Kampen AH, Wanders RJ, and Moerland PD (2012) Improving the description of metabolic networks: the TCA cycle as example. *FASEB J* **26**:3625–3636.

Tolson AH and Wang H (2010) Regulation of drug-metabolizing enzymes by xenobiotic receptors: PXR and CAR. *Adv Drug Deliv Rev* **62**:1238–1249.

Wada T, Gao J, and Xie W (2009) PXR and CAR in energy metabolism. *Trends Endocrinol Metab* **20**:273–279.

Wang H, Faucette S, Sueyoshi T, Moore R, Ferguson S, Negishi M, and LeCluyse EL (2003) A novel distal enhancer module regulated by pregnane X receptor/constitutive androstane receptor is essential for the maximal induction of CYP2B6 gene expression. *J Biol Chem* **278**:14146–14152.

Wang H and LeCluyse EL (2003) Role of orphan nuclear receptors in the regulation of drug-metabolising enzymes. *Clin Pharmacokinet* **42**:1331–1357.

Willson TM and Kliewer SA (2002) PXR, CAR and drug metabolism. *Nat Rev Drug Discov* **1**:259–266.

Xie W, Barwick JL, Downes M, Blumberg B, Simon CM, Nelson MC, Neuschwander-Tetri BA, Brunt EM, Guzelian PS, and Evans RM (2000a) Humanized xenobiotic response in mice expressing nuclear receptor SXR. *Nature* **406**:435–439.

Xie W, Barwick JL, Simon CM, Pierce AM, Safe S, Blumberg B, Guzelian PS, and Evans RM (2000b) Reciprocal activation of xenobiotic response genes by nuclear receptors SXR/PXR and CAR. *Genes Dev* **14**:3014–3023.

Zhou C, Poulton EJ, Grün F, Bammler TK, Blumberg B, and Eaton DL (2007) The dietary isothiocyanate sulforaphane is an antagonist of the human steroid and xenobiotic nuclear receptor. *Mol Pharmacol* **71**:220–229.

Zhou J, Febbraio M, Wada T, Zhai Y, Kuruba R, He J, Lee JH, Khadem S, Ren S, and Li S et al. (2008) Hepatic fatty acid transporter Cd36 is a common target of LXR, PXR, and PPARgamma in promoting steatosis. *Gastroenterology* **134**:556–567.

Address correspondence to: Dr. Hongbing Wang, Department of Pharmaceutical Sciences, University of Maryland School of Pharmacy, 20 Penn Street, Baltimore, MD 21201. E-mail: hwang@rx.umaryland.edu